Self-forming graphene/Ni patterns on sapphire utilizing the pattern-controlled catalyst metal agglomeration technique

Makoto Miyoshi, Yukinori Arima, Toshiharu Kubo, and Takashi Egawa

Citation: Appl. Phys. Lett. **110**, 013103 (2017);
View online: https://doi.org/10.1063/1.4973523
View Table of Contents: http://aip.scitation.org/toc/apl/110/1
Published by the American Institute of Physics

Articles you may be interested in

Fermi-level pinning of bilayer graphene with defects under an external electric field
Applied Physics Letters **110**, 011601 (2017); 10.1063/1.4973426

Impact of N-plasma and Ga-irradiation on MoS_2 layer in molecular beam epitaxy
Applied Physics Letters **110**, 012101 (2017); 10.1063/1.4973371

Universal conformal ultrathin dielectrics on epitaxial graphene enabled by a graphene oxide seed layer
Applied Physics Letters **110**, 013106 (2017); 10.1063/1.4973200

Resist-free fabricated carbon nanotube field-effect transistors with high-quality atomic-layer-deposited platinum contacts
Applied Physics Letters **110**, 013101 (2017); 10.1063/1.4973359

Direct synthesis of multilayer graphene on an insulator by Ni-induced layer exchange growth of amorphous carbon
Applied Physics Letters **110**, 033108 (2017); 10.1063/1.4974318

Fabrication and applications of multi-layer graphene stack on transparent polymer
Applied Physics Letters **110**, 041901 (2017); 10.1063/1.4974457

Scilight
Sharp, quick summaries illuminating the latest physics research
Sign up for FREE!

APPLIED PHYSICS LETTERS **110**, 013103 (2017)

Self-forming graphene/Ni patterns on sapphire utilizing the pattern-controlled catalyst metal agglomeration technique

Makoto Miyoshi,[a] Yukinori Arima, Toshiharu Kubo, and Takashi Egawa
Research Center for Nano Device and Advanced Materials, Nagoya Institute of Technology, Nagoya 466-8555, Japan

(Received 24 September 2016; accepted 19 December 2016; published online 3 January 2017)

We fabricated graphene/Ni patterns directly on sapphire substrates through a self-forming process utilizing the pattern-controlled catalyst metal agglomeration technique, which was accomplished via a thermal annealing process of rectangular Ni patterns preformed on thin amorphous carbon films on sapphire. It was confirmed that graphene films were synthesized along with the preformed Ni patterns as a result of the progress of Ni agglomeration. Notably, a few-layer graphene film was observed in specific areas along the periphery of the preformed Ni patterns. The self-forming graphene/Ni patterns showed ohmic conductivity with a contact resistance ranging from 4×10^4 to 7×10^4 Ω μm. *Published by AIP Publishing.* [http://dx.doi.org/10.1063/1.4973523]

Graphene is highly promising as a material for future high-frequency electronic and/or large-scale integrated circuit devices owing to its ballistic carrier transport properties.[1–4] Although there is a wide variety of graphene synthesis processes,[5–17] the development of substrate transfer-free processes is still very important for the practical use and mass production of graphene devices; therefore, some useful ideas for transfer-free techniques have been suggested.[18–29] Recently, we reported another transfer-free graphene synthesis process utilizing a catalyst metal agglomeration phenomenon.[26–28] According to our results, multilayer graphene films can be formed directly on insulating substrates simply by employing a thin metal film as an underlying catalyst film.[26–28] Most recently, we have reported that sapphire is an appropriate substrate for our transfer-free graphene synthesis technique[28] and that drain currents in transfer-free graphene transistors fabricated on sapphire were properly modulated with applied gate voltages.[28] Subsequently, we conceived the idea of applying our transfer-free technique to self-forming graphene devices. That is, if the metal agglomeration and transfer-free graphene synthesis progress at the same time by utilizing preformed catalyst metal patterns, self-forming graphene devices can be realized. In this letter, we report our first attempt on fabricating self-forming graphene devices by utilizing the pattern-controlled catalyst metal agglomeration technique.

Figure 1 shows schematics of the proposed self-forming graphene synthesis process. First, an amorphous carbon (a-C) film was deposited on a single-crystal *c*-face sapphire substrate by using the pulse arc plasma deposition (PAPD) technique,[17,26–28] in which the number of discharge pulses was maintained at 50. Then, the a-C film excluding the device areas was removed by dry etching using O_2 plasma in an ashing reactor. The etching conditions were as follows: the O_2 flow rate was 5 sccm, the reactor pressure was 35 Pa, and the input power was 30 W. Subsequently, a thin Ni film with a thickness of 20 nm was deposited on the a-C film by using the electron-beam (EB) evaporation technique, following which Ni patterns with a thickness of 300 nm were formed on the thin Ni film through the combination of photolithographic lift-off technique and EB evaporation. Finally, samples were annealed at 1000 °C for 5 min under nitrogen gas flow. During the thermal annealing, carbon atoms dissolve in the Ni films and then precipitate as graphene films almost simultaneously with the progress of the agglomeration of the thin Ni film. Basically, the metal agglomeration originates from the surface migration of metals, which occurs to decrease the surface energy. Therefore, the thick rectangular Ni patterns were placed to make the thin Ni films migrate toward the thick Ni patterns. Here, if the thick Ni patterns are usable as ohmic electrodes, the realization of self-forming graphene devices is expected. Square patterns of side 80 μm with 5-μm spacing were applied for the formation and evaluation of graphene/Ni patterns. Scanning electron microscopy (SEM) and high resolution transmittance

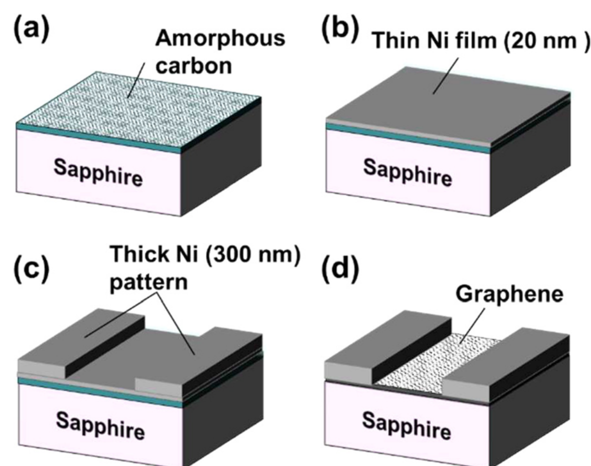

FIG. 1. Schematic illustrations of self-forming graphene/Ni patterns. (a) Amorphous carbon (a-C) film is deposited on sapphire using PAPD technique. (b) Thin Ni films (20 nm) are deposited on the a-C/sapphire. (c) Thick Ni (300 nm) patterns are formed on the thin Ni films. (d) After annealing, graphene films are directly formed in the area where the thin Ni films had existed.

[a]Author to whom correspondence should be addressed. Electronic mail: miyoshi.makoto@nitech.ac.jp. Telephone/Fax: +81-52-735-5092.

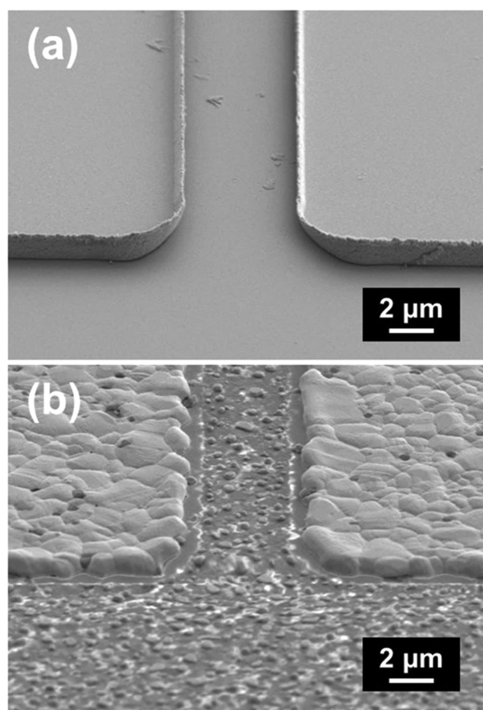

FIG. 2. Bird-view SEM images for samples (a) before and (b) after the thermal annealing.

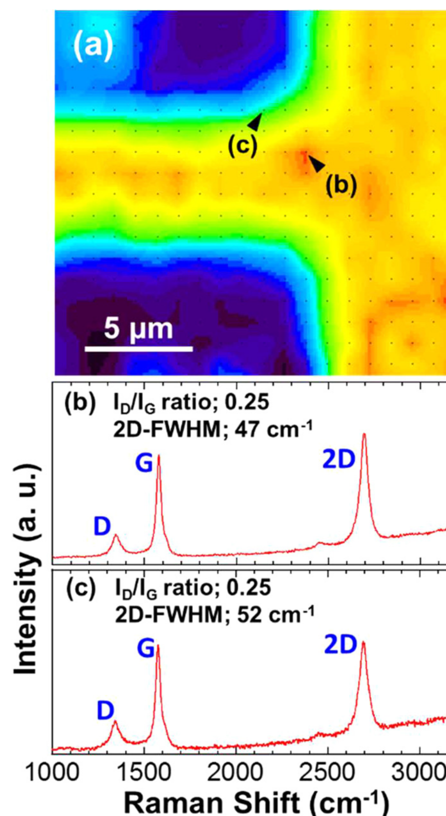

FIG. 3. (a) Raman map of integrated 2D band (2700 cm^{-1}) intensities for an annealed sample, in which the increase in the intensities corresponds to the change in color from dark blue to red. Typical Raman spectra for (b) an area around the middle area between the thick Ni patterns and (c) an area along the periphery of the thick Ni patterns.

electron microscopy (HR-TEM) were used for the microstructure analyses of the fabricated graphene/Ni patterns. To evaluate the crystal quality of graphene films, Raman scattering measurements were carried out, in which a 532-nm-wavelength solid-state laser with an output power of 10 mW was used as an excitation light source. Finally, the current–voltage (*I*–*V*) characteristics were measured using a semiconductor parameter analyzer.

Figures 2(a) and 2(b) show bird's-eye-view SEM images for a sample before and after the thermal annealing, respectively. After the thermal annealing, as can be seen in Fig. 2(b), many metallic particles were generated on the area where the thin Ni films had existed. This seemed to be consistent with our previous reports.[26–28] In addition, the observation results revealed another fact that the particles did not exist in specific areas along the periphery of the thick Ni patterns. This is probably because the thin Ni films adjacent to the thick Ni patterns migrated toward the thick Ni patterns without forming the metallic particles. This implies the possibility that the generation of the metallic particles may be suppressed by applying narrow distance Ni patterns. This concept will be one of our future plans. Fig. 3(a) shows a Raman map of integrated 2D band (2700 cm^{-1}) intensities taken for an annealed sample. Here, the increase in the intensities corresponds to the change in color from dark blue to red, and the 2D band in the Raman map indicates the existence of graphene.[29] From Fig. 3(a), it is obvious that graphene films were synthesized in the area where the thin Ni films had existed. It should be noted that the 2D band intensity detected in the area along the periphery of the thick Ni patterns was somewhat weaker than that around the middle area between the thick Ni patterns. Figs. 3(b) and 3(c) show typical Raman spectra for those two areas, in which the representative Raman parameters, integrated Raman intensity ratios of the D band to the G band (I_D/I_G ratio) and the full widths at half maximum of the 2D band peaks (2D-FWHMs), are also shown. These two parameters are considered useful indexes for evaluating structural disorders of graphene films.[29] The measured results indicate that the quality of graphene is not so different between the two above-mentioned areas. In addition, it was also confirmed that the measured Raman spectra and the derived parameters were almost consistent with the results obtained in our previous reports.[28] From these results, the difference of the 2D band intensity observed in the Raman map was speculated to be dependent mainly on the graphene thicknesses, rather than on the crystal quality. Fig. 4 shows typical cross-sectional HR-TEM images for the annealed sample. Here, the images seen in Figs. 4(a) and 4(b) were focused on an area around an agglomerated Ni particle, and the images seen in Figs. 4(c) and 4(d) were focused on an area around an edge of the thick Ni pattern. From these images, it was found that a few-layer graphene film was synthesized around the edge of the Ni pattern while multilayer graphene films were generated around the Ni particle in the same manner as in our previous reports.[26–28] Thus far, we have not determined the reason why the few-layer graphene was generated along the periphery of the thick Ni patterns. However, the self-forming graphene film generated around the patterned Ni might be prone to become a few-layer graphene film. Thus, we can expect that few-layer graphene films can be realized over the whole

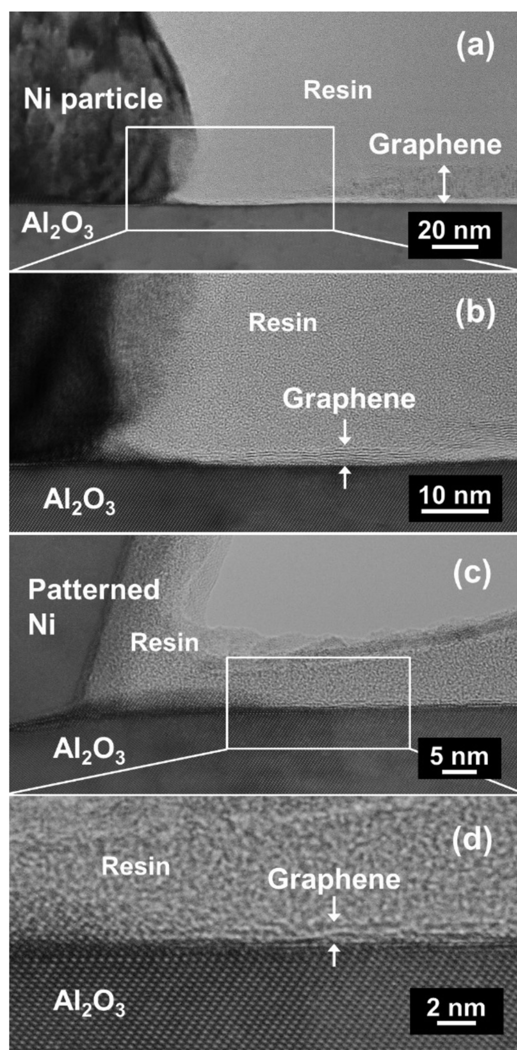

FIG. 4. Cross-sectional HR-TEM images for (a) and (b) a graphene film synthesized around an agglomerated Ni particle and (c) and (d) a graphene film synthesized around the edge of a thick Ni pattern.

area between the thick Ni patterns without the generation of the metallic particles by applying narrow distance Ni patterns.

Finally, we measured the electrical characteristics of the self-forming graphene film at room temperature. Fig. 5 shows the typical two-terminal $I-V$ characteristic of the self-forming graphene/Ni patterns measured using the thick Ni patterns as electrodes. The result clearly indicates that ohmic conductivity was achieved for the self-forming graphene/Ni patterns. The two-probe contact resistance of the self-forming graphene/Ni patterns was measured to range from 4×10^4 to 7×10^4 Ω μm, which is almost consistent with Ti/Al ohmic contacts fabricated in our previous study.[28]

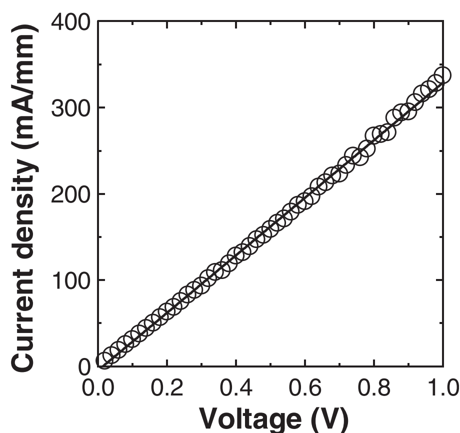

FIG. 5. Two-terminal *I-V* characteristics for a self-forming graphene/Ni pattern measured using thick Ni patterns as electrodes, which were formed as squares of side 80 μm with 5-μm spacing.

In summary, self-forming graphene/Ni patterns were fabricated directly on sapphire substrates by applying the pattern-controlled metal agglomeration technique. In addition to multilayer graphene films, which were observed in most areas with agglomerated Ni particles, we have confirmed that a few-layer graphene film was formed without the generation of Ni particles around specific areas along the periphery of the thick Ni patterns. The self-forming graphene/Ni patterns exhibited ohmic conductivity with contact resistance ranging from 4×10^4 to 7×10^4 Ω μm. In the future, we will conduct further research in order to realize transfer-free self-forming graphene devices using the pattern-controlled metal agglomeration technique.

This work was partially supported by a grant from the General Sekiyu Research & Development Encouragement & Assistance Foundation.

[1]K. S. Novoselov, A. K. Geim, S. V. Morozov, D. Jiang, Y. Zhang, S. V. Dubonos, I. V. Grigorieva, and A. A. Firsov, Science **306**, 666 (2004).
[2]Y. H. Wu, T. Yu, and Z. X. Shen, J. Appl. Phys. **108**, 071301 (2010).
[3]Y. M. Lin, C. Dimitrakopoulos, K. A. Tenkins, D. B. Farmer, H. Y. Chiu, A. Grill, and Ph. Avouris, Science **327**, 662 (2010).
[4]F. Schwierz, Nat. Nanotechnol. **5**, 487 (2010).
[5]I. Forbeaux, J. M. Themlin, and J. M. Debever, Phys. Rev. B **58**, 16396 (1998).
[6]K. V. Emtsev, A. Bostwick, K. Horn, J. Jobst, G. L. Kellogg, L. Ley, J. L. McChesney, T. Ohta, S. A. Reshanov, J. Röhrl, E. Rotenberg, A. K. Schmid, D. Waldmann, H. B. Weber, and T. Seyller, Nat. Mater. **8**, 203 (2009).
[7]M. Suemitsu and H. Fukidome, J. Phys. D: Appl. Phys. **43**, 374012 (2010).
[8]A. Ouerghi, A. Kahouli, D. Lucot, M. Portail, L. Travers, J. Gierak, J. Penuelas, P. Jegou, A. Shukla, T. Chassagne, and M. Zielinski, Appl. Phys. Lett. **96**, 191910 (2010).
[9]A. Reina, X. Jia, J. Ho, D. Nezich, H. Son, V. Blovic, M. S. Dresselhaus, and J. Kong, Nano Lett. **9**, 30 (2009).
[10]E. Kim, W. G. Lee, and J. Jung, Electron. Mater. Lett. **7**, 261 (2011).
[11]Y. Miyata, K. Kamon, K. Ohashi, R. Kitaura, M. Yoshimura, and H. Shinohara, Appl. Phys. Lett. **96**, 263105 (2010).
[12]M. Zheng, K. Takei, B. Hsia, H. Fang, X. Zhang, N. Ferralis, H. Ko, Y. L. Chueh, Y. Zhang, R. Maboudian, and A. Javey, Appl. Phys. Lett. **96**, 063110 (2010).
[13]K. S. Kim, Y. Zhao, H. Jang, S. Y. Lee, J. M. Kim, K. S. Kim, J. Ahn, P. Kim, J. Choi, and B. H. Hong, Nature **457**, 706 (2009).
[14]Y. Kim, W. Song, S. Y. Lee, C. Jeon, W. Jung, M. Kim, and C-Y. Park, Appl. Phys. Lett. **98**, 263106 (2011).
[15]J. Kim, M. Ishihara, Y. Koga, K. Tsugawa, M. Hasegawa, and S. Iijima, Appl. Phys. Lett. **98**, 091502 (2011).
[16]M. Keidar, A. Shashurin, J. Li, O. Volotskova, M. Kundrapu, and T. S. Zhuang, J. Phys. D: Appl. Phys. **44**, 174006 (2011).
[17]K. Fujita, K. Banno, H. R. Aryal, and T. Egawa, Appl. Phys. Lett. **101**, 163109 (2012).
[18]M. P. Levendorf, C. S. Ruiz-Vargas, S. Garg, and J. Park, Nano Lett. **9**, 4479 (2009).
[19]D. Kondo, S. Sato, K. Yagi, N. Harada, M. Sato, M. Nihei, and N. Yokoyama, Appl. Phys. Express **3**, 025102 (2010).
[20]Z. Yan, Z. Peng, Z. Sun, J. Yao, Y. Zhu, Z. Liu, P. M. Ajayan, and J. M. Tour, ACS Nano **5**, 8187 (2011).
[21]P. J. Wessely, F. Wessely, E. Birinci, U. Schwalke, and B. Riedinger, J. Vac. Sci. Technol., B **30**, 03D114 (2012).

[22]J. Kwak, J. H. Chu, J. Choi, S. Park, H. Go, S. Y. Kim, K. Park, S. Kim, Y. Kim, E. Yoon E, S. Kodambaka, and S. Kwon, Nat. Commun. **3**, 645 (2012).
[23]K. Gumi, Y. Ohno, K. Maehashi, K. Inoue, and K. Matsumoto, Jpn. J. Appl. Phys., Part 1 **51**, 06FD12 (2012).
[24]G. Pan, B. Li, M. Heath, D. Horsell, M. L. Wears, L. A. Taan, and S. Awan, Carbon **65**, 349 (2013).
[25]W. Kim, P. C. Debnath, J. Lee, J. H. Lee, D. Lim, and Y. Song, Nanotechnol. **24**, 365603 (2013).
[26]K. Banno, M. Mizuno, K. Fujita, T. Kubo, M. Miyoshi, T. Egawa, and T. Soga, Appl. Phys. Lett. **103**, 082112 (2013).
[27]M. Miyoshi, M. Mizuno, T. Kubo, T. Egawa, and T. Soga, Mater. Res. Express **2**, 015602 (2015).
[28]M. Miyoshi, M. Mizuno, Y. Arima, T. Kubo, T. Egawa, and T. Soga, Appl. Phys. Lett. **107**, 073102 (2015).
[29]D. Graf, F. Molitor, K. Ensslin, C. Stampfer, A. Jungen, C. Hierold, and L. Wirtz, Nano Lett. **7**, 238 (2007).